NeuroImage: Clinical 30 (2021) 102643

Contents lists available at ScienceDirect

NeuroImage: Clinical

journal homepage: www.elsevier.com/locate/ynicl

Latent patterns of task-related functional connectivity in relation to regions of hyperactivation in individuals at risk of Alzheimer's disease

Nick Corriveau-Lecavalier [a,b], M. Natasha Rajah [c,d], Samira Mellah [b], Sylvie Belleville [a,b,*]

[a] Research Center, Institut universitaire de gériatrie de Montréal, Montreal, Canada
[b] Department of Psychology, Université de Montréal, Montreal, Canada
[c] Department of Psychiatry, McGill University, Montreal, Canada
[d] Douglas Research Centre, Montreal, Canada

ARTICLE INFO

Keywords:
Functional connectivity
Hyperactivation
Mild cognitive impairment
Subjective cognitive decline
Task-related fMRI

ABSTRACT

The goal of this study was to assess how task-related hyperactivation relates to brain network dysfunction and memory performance in individuals at risk of Alzheimer's disease (AD). Eighty participants from the CIMA-Q cohort were included, of which 28 had subjective cognitive decline *plus* (SCD^+), as they had memory complaints and worries in addition to a smaller hippocampal volume and/or an *APOE4* allele, 26 had amnestic mild cognitive impairment (MCI) and 26 were healthy controls without memory complaints. Functional magnetic resonance imaging (fMRI) activation was measured during an object-location memory task. Seed-partial least square analyses (seed-PLS) were conducted in controls and in the SCD^+/MCI groups to yield sets of orthogonal latent variables (LVs) assessing the triple association between: i) seed activity in brain regions found to be hyperactive in individuals at risk of AD (left hippocampus, left superior parietal lobule, right inferior temporal lobe), ii) latent patterns of whole-brain task-related activation, and iii) associative memory performance. Three LVs in the SCD^+ and MCI groups (67.88% of total covariance explained) and two LVs in the controls (77.85% of total covariance explained) were significant. While controls and SCD^+/MCI groups shared a common pattern of memory-related connectivity, patterns of hyperactivation-networks interactions were unique to the clinical groups. Interestingly, higher hippocampal connectivity was associated with poorer memory performance whereas higher neocortical connectivity predicted better memory performance in SCD^+ and MCI groups. Our data provides empirical evidence that early dysfunction in brain activation and connectivity is present in the very early stages of AD and offers new insights on the relationship between functional brain alterations and memory performance.

1. Introduction

Early changes in brain function have been proposed to represent an early hallmark of Alzheimer's disease (AD) (Pasquini et al., 2019; Sperling et al., 2010, 2011). Interestingly, individuals in the early stages of AD show increased brain activation – a phenomenon known as hyperactivation – in regions vulnerable to AD. Increased task-related fMRI activation has been reported in patients with mild cognitive impairment (MCI) and subjective cognitive decline (SCD), compared to healthy controls (Celone et al., 2006; Clément and Belleville, 2010; 2012; Clément et al., 2010, 2013; Corriveau-Lecavalier et al., 2019, 2021; Erk et al., 2011; Rodda et al., 2009, 2011). Therefore, the presence of hyperactivation in specific brain regions could serve as an early signature of AD and may shed light on early brain dysfunction related to the disease.

Increasing knowledge about functional brain changes in AD shows that the disease not only targets specific brain regions but also impacts the functional integrity and connectivity of multiple brain networks (see Jacobs et al., 2013 for a *meta*-analysis). Hence it is plausible that hyperactivation found in brain regions vulnerable to the disease may be associated with altered patterns of functional connectivity in brain networks affected by AD. Preclinical studies and animal models suggest that early hyperactivation of specific brain regions could drive and/or be driven by dysfunction in neuronal networks (for a review, see Zott et al., 2018). This is consistent with the finding that hyperactivation occurs in brain areas that are part of large-scale networks vulnerable to the early

* Corresponding author at: Research Centre, Institut universitaire de gériatrie de Montréal, 4565 Queen-Mary Rd, Montreal, Quebec H3W 1W5, Canada.
E-mail address: sylvie.belleville@umontreal.ca (S. Belleville).

https://doi.org/10.1016/j.nicl.2021.102643
Received 13 October 2020; Received in revised form 18 March 2021; Accepted 19 March 2021
Available online 26 March 2021

pathophysiological processes of AD (Chhatwal et al., 2018; Jones et al., 2016, 2017; Franzmeier et al., 2020a, 2020b). For example, task-related hyperactivation has repeatedly been observed in the hippocampus (Berron et al., 2019; Celone et al., 2006; Corriveau-Lecavalier et al., 2019; Corriveau-Lecavalier et al., 2021, Dickerson et al., 2004; Dickerson et al., 2005; Huijbers et al., 2015, 2019; Kircher et al., 2007; Putcha et al., 2011) and temporo-parietal areas (Clément and Belleville, 2010; 2012; Clément et al., 2010, 2013; Corriveau-Lecavalier et al., 2019; Elman et al., 2014; Marks et al., 2017). These regions are integrated in functional brain networks known to be affected in AD, such as the default mode and the fronto-parietal/task-positive and dorsal attention networks (Chhatwal et al., 2018; Franzmeier et al., 2020a; Greicius et al., 2004; Jones et al., 2011, 2016, 2017; Schultz et al., 2017; Sepulcre et al., 2017; Franzmeier et al., 2019).

Thus, one important question is whether regional hyperactivation is associated with network dysfunction in individuals at risk of AD. This link would be plausible given that early neuronal hyperactivity is thought to originate in sites of early AD pathology accumulation (Bero et al., 2011; Busche et al., 2012, 2019; Wu et al., 2016). Abnormalities in brain activation might then propagate to functionally connected regions, orchestrating AD pathology through topological propagation in an activity-dependent manner (Bischof et al., 2019; Franzmeier et al., 2019, 2020a, 2020b; Kim et al., 2019; Vogel et al., 2020). However, the presence of hyperactivation in localized regions vulnerable to AD and brain network dysfunction have only been assessed separately and their relationship remains unknown. This study aims to assess the link between hyperactivation and network dysfunction in individuals with MCI and SCD. Individuals with MCI show signs of cognitive impairment and while they do not meet criteria for dementia, they are at high risk of developing the disease. Participants with SCD complain about poor memory but do not show signs of cognitive impairment. However, a significant proportion of these individuals will progress to MCI. Hence the study of individuals with MCI and SCD allows the assessment of brain alterations occurring in the early stages of AD, prior to a dementia diagnosis. Given that SCD is a heterogenous construct and that other causes unrelated to neurodegenerative disease can result in memory complaints, we used the recent SCD *plus* (SCD^+; Jessen et al., 2014, 2020) criteria, which suggest reliance on biomarkers that increase the likelihood of preclinical AD in individuals with SCD. Participants with SCD^+ had smaller hippocampal volumes and/or *APOE4* genotype.

Another important objective of this study is to better understand functional brain alterations underlying cognitive impairment in patients with SCD^+ and MCI. Task-related designs are of particular relevance to assess patterns of dysfunction in brain activation and connectivity, which may underlie cognitive impairment associated with the early phases of AD. Moreover, it has been suggested that the relationship between hyperactivation and cognitive performance could vary as a function of the brain regions, where hyperactivation is observed and/or disease stage (Jones et al., 2016, 2017; Leal et al., 2017; Marks et al., 2017). Thus, our goal was to assess if hyperactivation found in different brain areas differentially relates to patterns of functional connectivity and memory performance in individuals with SCD^+ and MCI. Associative memory is one of the first cognitive functions to decline in patients with AD (Atienza et al., 2011; Troyer et al., 2008). Thus, studying associative memory may help clarify the relationship between alterations in regional brain activation and connectivity, and cognitive impairment in individuals at risk of AD.

In summary, it is hypothesized that early hyperactivation is linked to patterns of functional connectivity in brain networks associated with higher-order cognitive functions, such as associative memory in people at risk of dementia. This altered hyperactivation-network interaction should be associated with differences in cognitive symptomatology of the disease. To test this hypothesis, a multivariate seed-based partial least square (seed-PLS; Krishnan et al., 2011; McIntosh and Lobaugh, 2004) analysis was used to assess between-group similarities and differences in the triple association between: i) seed activity in brain regions found to be hyperactive in individuals at risk of AD, ii) latent patterns of whole-brain task-related activation, and iii) associative memory performance in individuals with SCD^+, MCI or controls. Brain activation was measured during an object-location associative memory task. Regions of interest (ROI) chosen for seed activation were the left hippocampus, the right inferior temporal gyrus and the left superior parietal lobule. These regions were selected because they were found to be either hyperactive or hypoactive in participants with SCD^+ and MCI used for this study (Corriveau-Lecavalier et al., 2021) and were thus considered to represent potential candidates to reveal AD-related network dysfunction.

2. Materials and methods

2.1. Participants

The study included data from participants from the Consortium for the Early Identification of Alzheimer's disease-Quebec (CIMA-Q) cohort. CIMA-Q's main objective is to characterize a longitudinal observational cohort of>350 community-dwelling older men and women recruited from three Canadian cities (Montreal, Sherbrooke and Quebec City). The CIMA-Q cohort includes participants that are either 1) cognitively healthy without memory complaints, 2) cognitively healthy with SCD, 3) suffering from MCI, or 4) diagnosed with dementia due to probable AD. CIMA-Q collects clinical, cognitive, biological, radiological and pathological data from these participants in order to, 1) establish an early diagnosis of AD, 2) make a well-characterized cohort available to the scientific community, 3) identify therapeutic targets and interventions to prevent or slow cognitive decline and AD, and 4) support clinical studies (Belleville et al., 2019). Data for this study were obtained from 108 CIMAQ participants who completed the fMRI memory examination at baseline. fMRI activation in this subgroup was reported in Corriveau-Lecavalier et al. (2021). This study was approved by the CIMA-Q research committee as well as the *Comité mixte d'éthique de la recherche vieillissement-neuroimagerie* of the *Centre intégré universitaire de santé et de services sociaux du Centre-Sud-de-l'Île-de-Montréal*. All participants provided written informed consent prior to taking part in the study.

The SCD^+ classification was based on the Subjective Cognitive Decline Initiative (Jessen et al., 2014) criteria, which relies on the presence of genetic (i.e. *APOE* genotype) and brain imaging (i.e. brain atrophy on MRI) biomarkers as evidence for an increased risk of preclinical AD. The presence of SCD was determined based on the question ''Do you feel like your memory is becoming worse?'', of which three answers were possible: 1) No, 2) Yes, but it does not worry me, and 3) Yes, this worries me. To be categorized as SCD, participants had to report both memory complaints and worries (answer 3). In addition, SCD participants had to perform within normal ranges on standardized clinical tests (scores of $>$ 26 on the Montreal Cognitive Assessment or MoCA; Nasreddine et al., 2005; score of $\leq$ 3 for 0–7 years of education, $\leq$5 for 8–15 years, and $\leq$ 9 for 16 or more years on the Logical Memory subtest of the Wechsler, 1987) and a score of 0 on the Clinical Dementia Rating Scale or CDR (Morris, 1997). In order to meet biomarker-based criteria for SCD^+, participants also had to carry at least one *APOE4* allele and/or have smaller left or right hippocampal volume. Small hippocampal volume was determined to be one standard deviation below the group mean of the control group, which comprised cognitively healthy participants without memory complaints from the CIMA-Q cohort, who were matched for age, sex and education (see below). Of the 61 CIMA-Q SCD participants with available fMRI data, 28 met the criteria for SCD^+ and were retained for analysis, of which 10 were *APOE4* positive, 21 had smaller left or right hippocampal volumes, and 4 had both risk factors.

The MCI criteria were based on the NIA-AA workgroup (Albert et al., 2011). These criteria required the presence of 1) presence of memory complaints and worries, 2) objective cognitive decline based on

standardized clinical tests (scores between 20 and 25 on the MoCA; score of ≤ 2 for 0–7 years of education, ≤4 for 8–15 years, and ≤ 8 for 16 or more years on the Logical Memory subtest of the Wechsler Memory Scale), and 3) and a score of 0.5 on the CDR.

The control group included older adults without memory complaints, who performed within the normal range on standardized clinical tests (MoCA, Logical Memory and CDR; see criteria for SCD for cut-offs).

Inclusion criteria were being older than 65 years of age, living in the community, being able to understand, read, and write French or English, having sufficient auditory and visual acuity to participate to a neuropsychological assessment, and agreeing to the clinical procedure and to a blood test. Participants were excluded if they planned to move outside of Quebec in the next three years, had a central nervous central system disease (e.g. subdural hematoma, subarachnoid hemorrhage, active epilepsy, primary or metastatic brain cancer), intracranial brain surgery, history of addiction to alcohol, drugs or narcotics, daily consumption of benzodiazepines equivalent or higher than 1 mg of lorazepam taken orally, and/or an illness or condition that could compromise participation in the study. All participants met safety criteria for inclusion in an MRI study and were right-handed.

All participants underwent an extensive assessment to characterize them on clinical, physical and cognitive levels (see Belleville et al, 2019 for more details about the CIMA-Q assessments). Blood sampling was conducted to determine participants' *APOE* genotype. Blood samples were obtained under fasting conditions (~10 h) and were processed immediately after the clinical assessment (10–30 min) or frozen at −80 °Cs.

2.2. fMRI task and procedure

The memory task has been described in a separate publication (Belleville et al, 2019; Corriveau-Lecavalier et al., 2021). Brain activation was acquired during a 10-minute in-scan encoding phase of a memory task. Participants were exposed to 78 coloured pictures of common objects belonging to one of six semantic categories (musical instruments, animals, fruits and vegetables, kitchen tools, sports gear and food) and 39 grey squares (control condition). Participants were asked to memorize the stimuli, as well as their position on the screen, and pay attention to the grey squares without memorizing them. To ensure that participants kept their attention on the task, they were asked to press a button on a remote control with their right hand when the stimulus was presented (picture or grey square). Stimuli were displayed on a black background for three seconds in one of four quadrants on a computer screen (top left; top tight; bottom left; bottom right) with an inter-stimuli interval varying from 500 to 18,500 ms. The order of presentation of the stimuli was randomized across participants. Instructions were displayed prior to the encoding phase.

Retrieval was done in a separate room 10 min following the scanning session. Participants were presented with the 78 previously studied pictures and 39 new pictures, one at a time at the center of a computer screen. For each picture, participants were asked to indicate whether they had seen the picture during the encoding phase or not by pressing ''Yes'' or ''No'' on a keyboard. If a picture was identified as previously seen, the participant had to indicate in which quadrant they had seen the stimulus using a keypad with buttons identified according to the locations on the four-position grid matching the visual display. There was an unlimited time to provide a response. The order of presentation of the stimuli differed from the encoding phase and was randomized across participants. To ensure participants understood the procedure, they performed a short practice of the task in a mock MRI with a reduced number of stimuli that differed from those used in the task.

2.3. Image acquisition

Data acquisition was performed at four different sites according to local scanning capacity (Unité de neuroimagerie fonctionnelle, Montreal, $N = 42$; Montreal Neurological Institute, Montreal, $N = 18$; Centre intégré en neuroimagerie et stimulation de Québec, Quebec City, $N = 14$; Centre de recherche du CHUS, Sherbrooke, $N = 6$). The CIMA-Q scanning protocol is referred to as the Canadian Dementia Imaging Protocol (Duchesne et al., 2019; www.cdip-pcid.ca). Image acquisition was performed using Siemens Healthcare (TrioTim) or Philips Medical Systems (Achieva and Ingenia) scanners with a magnetic field of 3 Tesla. Sequences were harmonized between the sites of the MRI scan to optimize image quality between manufacturers/types of scan. Quality control procedures were performed monthly to ensure cross-scan comparability. Briefly, T1 images were acquired in sagittal orientation, with a time of echo (TE) of 3.3 milli-seconds (mm) (Philips) or 2.98 ms (Siemens), a time of repetition (TR) of 2300 ms, a flip angle of 9°, a voxel size of 1 × 1 × 1 mm, and a matrix and field of view (FOV) of 256 × 248 mm. fMRI images were acquired according to the anterior-posterior commissure (AC-PC) orientation minus 20°, using echo-planar imaging (EPI) sequences sensitive to blood oxygen level-dependant (BOLD) contrast, with an inter-slice gap of 0.3 mm, a TE of 25 ms, a TR of 2500 ms, a flip angle of 9°, a voxel size of 3 × 3 × 3 mm, a FOV of either 240 × 240 mm (Phillips) or 222 × 222 mm (Siemens), and a matrix of either 80 × 80 mm (Phillips) or 74 × 74 mm (Siemens). The interested reader can consult Supplementary Materials 1 for additional details about acquisition parameters.

2.4. fMRI preprocessing

Individual functional images were preprocessed using Statistical Parametric Mapping 12 (SPM12; Wellcome Department of Imaging Neuroscience, Institute of Neurology, London, England) typical pipeline steps. The first four volumes of the run were discarded to exclude artefacts due to excessive movement. Functional images were unwrapped and realigned to median volume to create a mean image for every subject. The mean functional image was then coregistered to the corresponding anatomical T_1-weighted image, corrected for within-run movement and normalized to the Montreal Neurological Institute template with a voxel size of 3 × 3 × 3 mm. Images were smoothed by applying an 8 mm full width at half maximum (FWHM) Gaussian kernel. A high-passed filter (128 s) was applied to remove low-frequency signal drifts. Head motion was examined with the Motion Fingerprint toolbox (Wilke, 2012, 2014). Subjects were excluded from analysis if they had a total displacement of > 3 mm or a framewise displacement of > 1 mm during the functional run, and/or failed quality control based on visual inspection of motion artefacts in brain activation and/or abnormal signal intensity ($N = 9$).

2.5. Anatomical MRI

Hippocampal volume segmentation was done using *FreeSurfer* 5.3 traditional pipeline steps (Dale et al., 1999). Raw hippocampal volumes were extracted and individually corrected for intracranial volume and used to assess whether the participants met the hippocampal volume criteria for SCD^+ classification. White matter lesions were calculated by segmenting the T_1 and FLAIR images using a patch-based method (*volbrain*; http://volbrain.upv.es/) and expressed as a percentage of total brain volume.

2.6. Selection of regions of interests

Regions of hyperactivation were selected as seeds for multivariate analyses based on findings from a separate publication from our group using the same sample and fMRI task-related activation (Corriveau-Lecavalier et al., 2021). Analyses from this study included between-group comparisons (SCD^+, MCI, controls) of the correct associative encoding activation, meaning the activation associated with the encoding of items that were both correctly recognized and positioned in the post-scan recognition phase. Three regions were found to show

higher levels of brain activation (i.e., hyperactivation) in individuals with SCD$^+$ compared to the control group, while controlling for age, sex, scanning site and white matter lesions. These regions of hyperactivation were the left hippocampus (MNI coordinates X = -30, Y = –22, Z = -13), left superior parietal lobule (also found to be hypoactive in MCI; MNI coordinates X = -18, Y = -61, Z = 47), and right inferior temporal lobe (MNI coordinates X = 45, Y = −58, Z = −13) (See Fig. 1). The extent of each seed was 3 × 3 × 3 mm. Assessment of multicollinearity between seed activity in regions of interest was performed using Pearson correlations in the whole sample and within each separate group (Control, SCD$^+$, MCI). Correlation coefficients indicated that activation of seeds of interest was not collinear (ranging from −0.11 to 0.44).

2.7. Statistical analyses

2.7.1. Sociodemographic and behavioural measures

Between-group differences on sociodemographic measures were assessed with one-way ANOVAs and Tukey's tests for post-hoc comparisons for continuous variables, and chi square analysis for categorical variables.

To assess post-scan memory performance, an associative memory score was computed with the following = *correct sources*/(*wrong sources* + *false alarms*), where *correct sources* is the number of old items that were correctly recognized with their accurate position, *wrong sources* is the number of old items that were correctly recognized without their position, and *false alarms* is the number of new items that were falsely recognized. A positive asymmetric distribution was revealed for this variable using the Kolmogorov-Smirnov test and thus group differences on the associative memory score were assessed using a Kruskal-Wallis one-way ANOVA, with the Mann-Whitney *U* test for post-hoc comparisons.

2.7.2. Multivariate PLS analyses

Multivariate analyses of task-related brain activation and connectivity were carried out using PLS software (Krishnan et al., 2011; McIntosh and Lobaugh, 2004) implemented in MATLAB 9.4. Multivariate seed-based PLS analyses were used to assess the three-way associations between: 1) seed activity in regions of interest, 2) whole-brain activity associated with associative memory encoding, and 3) associative memory scores. Two separate PLS-analyses were performed: one including the control group, and another with the SCD$^+$ and MCI groups.

The PLS analysis consists in the decomposition of a cross-correlation matrix between two data matrices that is submitted to singular value decomposition (SVD). The first data matrix contained event-related fMRI data that was obtained during the encoding of successfully recognized and positioned items, which was deemed to reflect successful associative memory. Of note, this activation was not contrasted to activation associated with a control condition (i.e. gray squares), since PLS utilizes first-level preprocessed images. Associative memory-based fMRI events were stored in a data matrix, where the rows were organized so that events were nested within each participant, and participants were nested within group (if the analysis included more than one group). Columns of the matrix contained the average signal for the associative memory-based events (collapsed across correct trials) for each voxel in the brain at each of the seven time lags after the event onset, where each lag represented one time of repetition (TR; 2.5 s). In other words, this matrix contained fMRI data spanning 17.5 s after the event onset (columns) for each participant (rows). This fMRI data matrix was then cross-correlated with a second, similarly organized matrix containing activation values for each seed of interest, which averaged from lags 2 to 5, as well as an associative memory score for each participant. As such, this matrix contained activation of seeds of interest and associative memory performance (columns) for each participant (rows). Thus, this seed-PLS connectivity analysis may be described as activation-based rather than time-series-based, as it is the case with more traditional connectivity methods. The resulting cross-correlation matrix for each PLS analysis was submitted to a SVD, which yields a set of orthogonal Latent Variables (LVs) that is equal to the number of groups by seed/condition of interest (4 in controls; 8 in SCD$^+$/MCI). LVs can be broken down into three components: 1) a singular value indicating the significance of the LV as well as the covariance accounted by this particular LV; 2) a correlation profile that depicts how whole-brain activation correlates with seed activity and memory performance for each group; 3) a singular image indicating the pattern of whole-brain connectivity accounted by the LV with positive and negative salience regions.

Significance of LVs was tested using 1000 permutation tests on singular values. Bootstrapping was used to yield a bootstrap ratio (BSR) reflecting the reliability of voxel activation contributing to a given LV (500 iterations; minimum of 20 mm^3 per cluster; significance threshold set at BSR of ± 3, equivalent to $p = 0.002$). The number of permutation tests and bootstrap samples were determined based on previous studies that assessed latent patterns of memory-related activation and connectivity in aging and AD using PLS software (Ankudowich et al., 2016, 2017, 2019; Elshiekh et al., 2020; Rabipour et al., 2020).

An important aspect to keep in mind is that the pattern of whole-brain activation represented by a given LV is symmetrically reflected by the correlation profile. Salience and weights of brain regions identified by a given LV can be either positive or negative and indicate whether activation of the voxels relate positively or negatively with the correlation profiles. Thus, activation with a positive weight (warm colors on brain rendering) correlates positively with a positive correlation profile and negatively with a negative correlation profile. Since each LV reflects a symmetrical pairing of correlation profiles, the opposite would also be true: activation in a brain region with negative weights (cool-colored on brain rendering) correlates negatively with a positive correlation profile and positively with a negative correlation profile. Thus, interpretation of results should rely on the relationship between the LVs and seed activation/performance, rather than its directionality.

The SVD also provides individual brain scores for each LV, which reflect the extent to which an individual is represented by the pattern

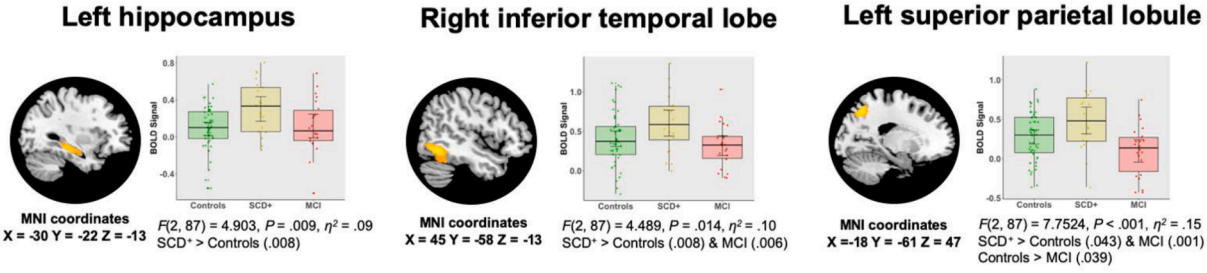

Fig. 1. Regions of interest selected as seeds for multivariate analyses, based on a separate between-group comparison of task-related activation (Corriveau-Lecavalier et al., submitted). The analysis of task-related activation included participants with 12 events or more, while controlling for age, sex, scanning site and white matter lesions.

expressed by the given LV. Brain scores were used for post-hoc analyses, as described below.

2.7.3. Assessment of potential effects of variables of non-interest

Given that the PLS analysis does not allow to directly control for confounding variables, we conducted univariate post-hoc analyses to ensure that our results were not driven by interindividual characteristics and head movement parameters, i.e. age, sex, site of scan, white matter lesion burden, total displacement and framewise displacement. Separate ANOVAs and linear regressions were performed to assess the effect of categorical variables (sex, site of scan) and continuous variables (age, white matter lesion burden, head motion parameters) on brain scores for each significant LV.

3. Results

3.1. Sociodemographic, clinical, and behavioral performance

Sociodemographic, clinical and neuropsychological data are summarized in Table 1. Groups were comparable on sex and *APOE4* distribution, years of education, total white matter lesions and head motion parameters. Participants in the MCI group performed slightly worse on the associative memory task than controls and the SCD$^+$ group, but the difference did not reach significance ($P = .091$ in both cases). Performance of the SCD$^+$ group did not differ from that of controls ($P = .591$). Individuals with MCI were significantly older than controls but comparable to participants with SCD$^+$, who did not differ from controls. Unsurprisingly, individuals with MCI had significantly lower scores on the MoCA than controls and SCD$^+$, and lower scores on Logical Memory tests than controls. Individuals with SCD$^+$ performed as well as controls on the MoCA and Logical Memory tests. SCD$^+$ and MCI groups had significantly smaller left and right hippocampal volumes than controls.

3.2. Multivariate functional connectivity analyses

Seed-PLS analysis revealed two significant LVs for controls and three significant LVs for individuals with SCD$^+$/MCI. Singular images (positive and negative salience regions) and correlation profiles for each significant LV are displayed in Fig. 2 (controls) and Fig. 3 (SCD$^+$/MCI). Summary statistics of correlations profiles (*r*, confidence intervals) are reported in Table 2. A list of regions highlighted by the significant LVs can be found in Supplementary Materials 2. Of note, PLS analyses were repeated while excluding *APOE4* carriers from the control group, and in the SCD$^+$ and MCI groups separately. These additional analyses yielded very similar results and can be found in Supplementary Materials 3.

Table 1
Sociodemographic, clinical, genetic, behavioural and structural imaging data.

	Controls	SCD$^+$	MCI	*P*-values (main group effect)
Participants (N)	26	28	26	–
Age (SD)	71.07 (4.47)	73.23 (5.21)	75.73 (5.01)[a]	$P = .004$
Sex, *M/F*	7, 19	15, 13	12, 14	$P = .127$
Education (SD)	15.73 (3.49)	15.46 (3.70)	15.20 (3.27)	$P = .864$
MoCA (SD)	28.35 (1.47)	27.68 (1.33)	24.96 (2.25)[b, c]	$P < .001$
Logical Memory Delayed Recall (SD)	14.65 (4.52)	12.68 (3.69)	11.00 (4.51)[a]	$P = .011$
APOE4 carriers (%)	5 (19.23)	10 (35.71)[b]	11 (42.31)[a]	$P = .071$
Associative memory score	2.29 (1.33)	2.18 (1.46)	1.62 (1.56)	$P = .214$
Left hippocampal volumes (SD)	0.29 (0.05)	0.24 (0.03)[b]	0.23 (0.05)[b, c]	$P < .001$
Right hippocampal volumes (SD)	0.30 (0.05)	0.24 (0.04)[b]	0.24 (0.05)[b, c]	$P < .001$
Total white matter lesions (SD)	0.7 (0.95)	0.64 (1.04)	0.4 (0.47)	$P = .416$
Mean total displacement (mm)	1.35 (0.88)	1.18 (0.67)	1.04 (0.64)	$P = .300$
Mean framewise displacement (mm)	0.16 (0.06)	0.17 (0.07)	0.19 (0.09)	$P = .587$

MoCA = Montreal Cognitive Assessment; Hippocampal volumes were corrected for intracranial volume; [a]$P < 0.01$ compared to Controls; [b]$P < 0.001$ compared to Controls; [c]$P < 0.001$ compared to SCD$^+$.

3.2.1. Patterns of connectivity in controls

3.2.1.1. LV1 in controls (LV1CTL). LV1CTL ($P < .001$, 51.32% variance explained) included a large number of positive salience regions mostly from the default mode and fronto-parietal brain networks bilaterally, as well as several other occipital, precentral, postcentral, subcortical and cerebellar regions. Negative salience regions only included small clusters located in the insula, midbrain and posterior cerebellum. The correlation profiles indicated significant positive correlations between this LV and the left superior parietal and right inferior temporal seeds, but no significant association with left hippocampal activity and memory performance.

3.2.1.2. LV2 in controls (LV2CTL). LV2CTL ($P = .036$, 26.47% variance explained) included positive saliences regions mostly in frontal, temporal and cerebellar areas bilaterally, as well as small occipito-parietal and subcortical clusters. Negative salience regions were mostly frontal regions bilaterally, with small clusters in the right superior temporal gyrus and the right cuneus. Assessment of correlation profiles indicated a positive association between this LV and hippocampal activity and memory performance, and no significant correlation with left superior parietal and right inferior temporal seed activity.

3.2.2. Patterns of connectivity in SCD$^+$/MCI

3.2.2.1. LV1 in clinical groups (LV1CLI). Similarly to controls, LV1CLI in SCD$^+$/MCI ($P < .001$, 30.16% variance explained) included positive salience regions encompassing areas from the default mode and fronto-parietal networks bilaterally, in addition to occipital, subcortical and cerebellar areas. Negative salience regions mostly included ventral occipito-temporal areas bilaterally, as well as frontal inferior gyri, and subcortical and cerebellar areas. Examination of correlation profiles showed positive association between this LV and left parietal and right inferior temporal seed activity but no correlation with left hippocampal activity in both SCD$^+$ and MCI groups. However, groups differed in that the LV was positively correlated with memory performance in SCD$^+$, but not in the MCI group.

3.2.2.2. LV2 in clinical groups (LV2CLI). LV2 ($P = .008$, 23.06% variance explained) included positive salience regions exclusively circumscribed to right prefrontal areas (cingulate gyrus, inferior and middle frontal gyrus). Negative salience regions were mostly situated in prefrontal, ventral occipito-temporal and cerebellar regions bilaterally, in addition to small dorsal parietal clusters bilaterally. Correlation profiles indicated a negative correlation between this LV and left hippocampus activity in both SCD$^+$ and MCI groups. However, groups differed in that this LV was positively correlated with the right inferior temporal activity and memory performance in individuals with SCD$^+$, whereas it was negatively correlated with the left superior and right inferior temporal seed activity and unrelated to performance in individuals with MCI.

3.2.2.3. LV3 in clinical groups (LV3CLI). LV3 ($P = .046$, 14.66% variance explained) identified positive salience regions, mostly in fronto-parietal areas bilaterally (including the insulas), and to a lesser extent, left temporal and cerebellar regions. Negative salience regions included almost exclusively temporal and subcortical areas bilaterally, in

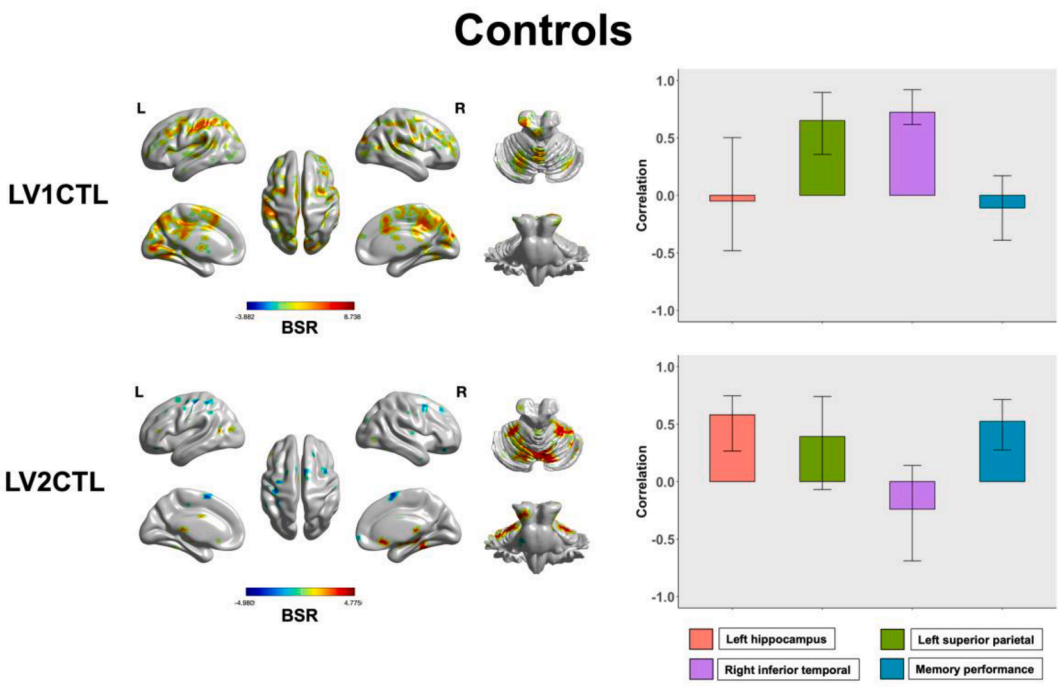

Fig. 2. Singular images and correlation profiles for the two latent variables (LV) found significant in the control group. Positive salience regions are illustrated in orange to yellow (left) and negative salience regions are illustrated in blue (middle) with a bootstrap ratio (BSR) threshold set at ± 3. Error bars in the correlation profiles graphics (right) express confidence intervals (95%). As a reminder, the salience and weights of brain regions identified by a given LV indicate whether activation of the voxels relate positively or negatively with the correlation profiles. Activation with a positive weight correlates positively with a positive correlation profile and negatively with a negative correlation profile. In the same way, activation with negative weights correlates negatively with a positive correlation profile and positively with a negative correlation profile. (For interpretation of the references to colour in this figure legend, the reader is referred to the web version of this article.)

addition to small clusters in the prefrontal lobe and cerebellum bilaterally. Examination of the correlation profiles indicated significant correlations almost only within the MCI group, in which this LV was negatively correlated with left hippocampal activity and left superior parietal lobule activity, and positively correlated with right inferior temporal activity and memory performance. Only a positive correlation between this LV and left superior parietal activity was found significant in participants with SCD^+.

3.3. *Effect of variables of non-interest*

Univariate post-hoc analyses revealed no significant effect of age, sex, site of scan, white matter lesion burden, total displacement and framewise displacement on brain scores for each significant LV, either in the control or SCD^+/MCI group.

4. Discussion

The primary objective of this study was to assess how regional hyperactivation in brain regions vulnerable to AD relates to multivariate patterns of functional connectivity in individuals with SCD^+ and MCI during an object-location associative memory task. The second objective was to examine how these patterns of hyperactivation networks relate to associative memory performance, and more precisely, if these associations differ depending on the brain area where hyperactivation is located and/or disease stage. The first PLS analysis was conducted in controls and yielded two significant LVs, which accounted for a total of 77.85% of covariance and reflected typical healthy memory-related patterns of connectivity. The second PLS analysis was conducted in clinical groups and showed three significant LVs, which explained a total of 67.88% of covariance altogether. These analyses revealed a set of compensatory and pathological connectivity patterns that vary depending on the area of the brain where hyperactivation is found and group membership. The following paragraphs summarize the main findings and discuss the implications of the results.

The PLS analysis conducted in controls should be interpreted with caution as the seeds of interest were selected based on regions of hyperactivation in the clinical groups. For this reason, the patterns identified may not fully reflect the memory networks that would typically be recruited in this group. Nevertheless, it is interesting that LV1CTL identified a set of positive salience regions from the default mode and fronto-parietal networks as well as cerebellar areas, which correlated positively with left superior parietal and right temporal activity. Furthermore, LV2CTL identified a fronto-temporo-cerebellar network, which correlated positively with left hippocampal activity and supports better memory performance. Both networks comprised brain regions typically involved in associative memory tasks (LV1CTL) (Benoit and Schacter, 2015) and/or positively related to memory performance (LV2CTL).

LV1CLI in SCD^+ and MCI groups identified mostly positive salience regions that included brain areas from the default mode and fronto-parietal networks. Activation of these regions positively correlated with left superior parietal and right inferior parietal activity. This pattern is very similar to what was found in the first LV identified in controls (LV1CTL). Contrary to what was found in the control and MCI groups, this hyperactivation-network was positively correlated with memory performance in the SCD^+ group only. This means that a higher level of left superior parietal and right inferior temporal activation and stronger connectivity within this network were associated with better memory in this group.

LV2CLI showed mostly negative salience regions in a fronto-temporo-cerebellar network, which correlated negatively with left hippocampal activity and positively with memory performance in SCD^+. This suggests that higher hippocampal hyperactivation and connectivity of the negative salience regions of this network are related to poorer memory performance. In addition, there were some areas of positive

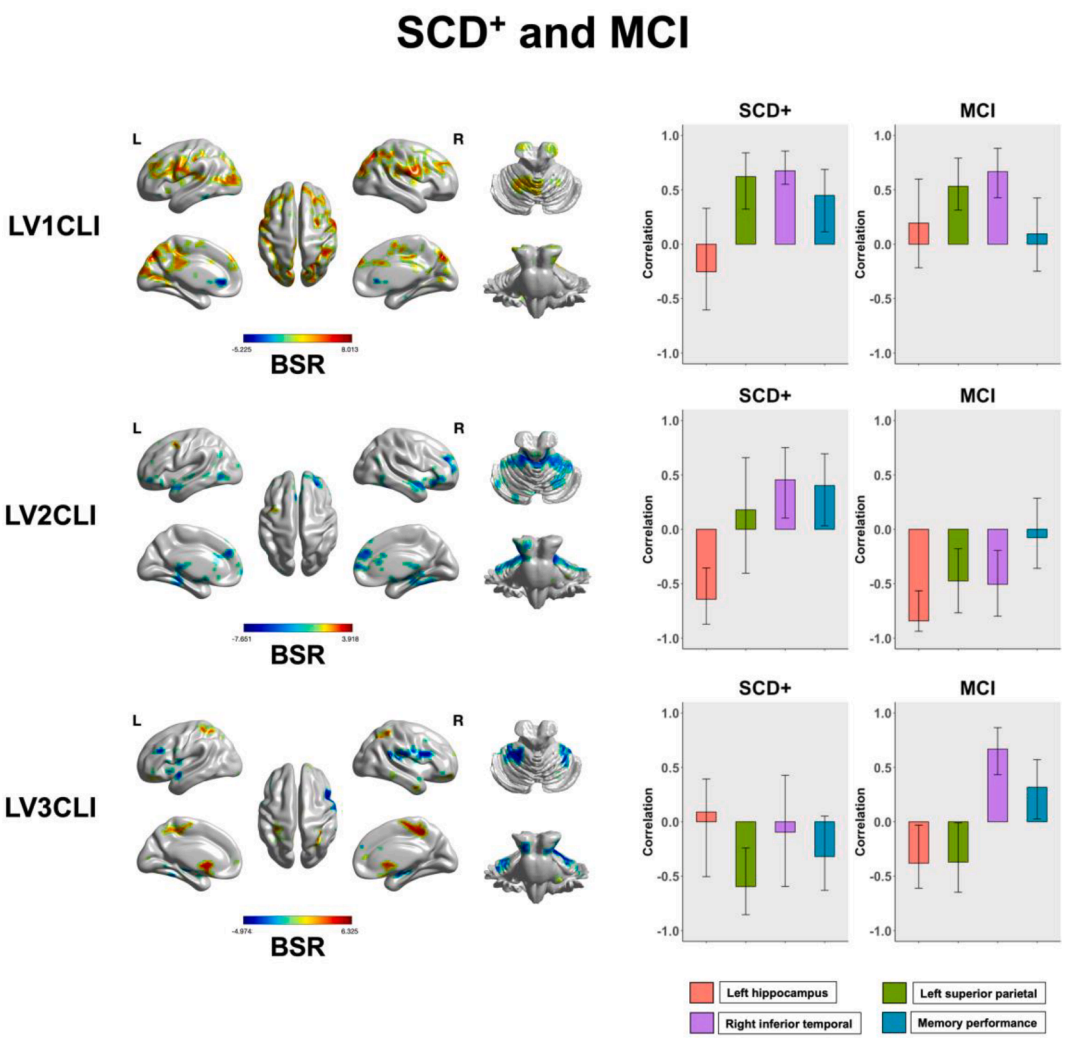

Fig. 3. Singular images and correlation profiles for each significant latent variable (LV) for the SCD^{+}/MCI groups. Positive salience regions are illustrated in orange to yellow (left) and negative salience regions are illustrated in blue (middle) with a bootstrap ratio (BSR) threshold set at ± 3. Error bars in the correlation profiles graphics (right) express confidence intervals (95%). The salience and weights of brain regions identified by a given LV indicate whether activation of the voxels relate positively or negatively with the correlation profiles. Activation with a positive weight correlates positively with a positive correlation profile and negatively with a negative correlation profile. Furthermore, activation in a brain region with negative weights correlates negatively with a positive correlation profile and positively with a negative correlation profile. (For interpretation of the references to colour in this figure legend, the reader is referred to the web version of this article.)

salience in right frontal areas, where activation was positively associated with left parietal and right temporal seed activity and memory performance.

LV3CLI identified a network involving fronto-parietal regions bilaterally (positive salience regions), as well as fronto-temporal areas (negative salience regions). For this particular LV, significant patterns of correlations were almost exclusively found in the MCI group. In that group, positive salience regions were associated with right inferior temporal activation and better memory performance, whereas the negative salience regions were associated with left hippocampal and superior parietal activation and poorer memory performance. In the SCD^{+} group, activation of negative salience regions was associated with left superior parietal activity but was not related to memory or activation of other regions.

An interesting finding arising from the connectivity patterns found in clinical groups concerns the remarkable contrast in the relationship between patterns of connectivity and memory performance for hippocampal versus neocortical activation. On the one hand, left hippocampal activation and its connectivity with fronto-temporal areas were associated with poorer memory in both SCD^{+} (LV2CLI) and MCI (LV3CLI) groups. On the other hand, the left superior parietal activation and right inferior temporal activation and their connected networks were associated with better memory in SCD^{+} (for the both networks; LV1CLI & LV2CLI) and MCI (for the fronto-temporal network; LV3CLI) groups. These findings may help clarify whether hyperactivation and hyperconnectivity reflect compensatory processes or pathophysiological mechanisms. One hypothesis is that the nature of hyperactivation may vary as a function of the brain region where it is observed (Leal et al., 2017; Marks et al., 2017). Hippocampal hyperactivation and hyperconnectivity was suggested to reflect AD-related pathophysiological mechanisms (Bakker et al., 2012, 2015; Berron et al., 2019; Huijbers et al., 2019; Richetin et al., 2020; Putcha et al., 2011), a view consistent with our observation as it is related with poorer memory performance. In turn, hyperactivation in parietal and temporal regions may reflect compensatory mechanisms (Belleville et al., 2011, 2021; Corriveau-Lecavalier et al., 2019; Elman et al., 2014). This view is supported by our finding that higher left superior parietal and right inferior temporal activity and stronger connectivity between these regions and associated networks were correlated with better memory performance. This indicates that greater recruitment of these neocortical areas and increased connectivity in these networks may underlie compensatory mechanisms, which is a new finding that is absent from

Table 2
Summary of correlation profiles yielded by significant LVs.

		Controls		
	Variable of interest	*r*	Upper bound	Lower bound
LV1CTL	Left hippocampal activation	−0.05	0.50	−0.48
	Left superior parietal activation	*0.65	0.90	0.36
	Right inferior temporal activation	*0.72	0.92	0.62
	Associative memory performance	−0.11	0.17	−0.39
LV2CTL	Left hippocampal activation	*0.58	0.75	0.26
	Left superior parietal activation	0.39	0.74	−0.07
	Right inferior temporal activation	−0.24	0.14	−0.69
	Associative memory performance	*0.52	0.71	0.27

		SCD+/MCI					
		SCD+			MCI		
	Variable of interest	*r*	Upper bound	Lower bound	*r*	Upper bound	Lower bound
LV1CLI	Left hippocampal activation	−0.25	0.33	−0.60	0.19	0.60	−0.22
	Left superior parietal activation	0.62*	0.84	0.32	0.53*	0.79	0.31
	Right inferior temporal activation	0.67*	0.86	0.55	0.68*	0.88	0.43
	Associative memory performance	0.45*	0.69	0.11	0.10	0.43	−0.25
LV2CLI	Left hippocampal activation	−0.64*	−0.36	−0.87	−0.84*	−0.57	−0.94
	Left superior parietal activation	0.18	0.66	−0.40	−0.48*	−0.18	−0.77
	Right inferior temporal activation	0.46*	0.75	0.10	−0.51*	−0.19	−0.80
	Associative memory performance	0.40*	0.69	0.03	−0.08	0.29	−0.36
LV3CLI	Left hippocampal activation	0.09	0.39	−0.50	−0.38*	−0.031	−0.61
	Left superior parietal activation	−0.60*	−0.24	−0.85	−0.37*	−0.01	−0.65
	Right inferior temporal activation	−0.10	0.43	−0.59	0.69*	0.86	0.43
	Associative memory performance	−0.32	0.05	−0.63	0.32*	0.57	0.03

* Significant correlation.

prior studies assessing the relationship between neocortical activation and cognitive performance.

Another finding worth discussing relates to the differences observed between SCD$^+$ and MCI groups. Indeed, left parietal activation and its related connectivity patterns showed opposite directions of association with memory performance when examining SCD$^+$ and MCI groups, as it is associated with better memory performance in the former (LV1CLI) but with poorer memory in the latter (LV3CLI). This is consistent with the hypothesis mentioned above that parietal hyperactivation/hyperconnectivity found in the early phase of the disease may reflect compensatory mechanisms and contribute to the maintenance of cognition in SCD$^+$. As individuals with MCI begin to experience objective memory problems, the pattern may reflect a compensation attempt and/or compensation failure in patients suffering from an accumulation of disease-related neuropathology. Thus, it is plausible that a portion of people with MCI have a similar pattern to those with SCD$^+$, meaning a relatively higher level of parietal activation/connectivity, but without its associated cognitive benefit. This is in line with the ''Cascading Network Failure'' model (Jones et al., 2016, 2017), which proposes that parietal areas could serve as a transient compensatory role in the early phase of the disease, before triggering downstream AD-related pathological processes with increased pathoprogression.

Although this study did not include biomarkers of AD, our findings concur with several studies and models relating the fundamental pathophysiological processes of AD functional connectivity disruption. For example, our finding that activation of the left hippocampus and its associated connectivity correlated with poorer memory performance in clinical groups is consistent with prior reports showing that abnormal levels of amyloid and tau alter hippocampal activation/connectivity in transgenic mice and humans at risk of AD (Berron et al., 2019; Busche et al., 2019; Hallinan et al., 2019a, 2019b; Huijbers et al., 2019; Mormino et al., 2012; Zott et al., 2019), thus resulting in poorer memory performance (Bai et al., 2009; Richetin et al., 2020; Putcha et al, 2011; Yassa et al., 2011).

Our findings have implications for early identification and intervention. To our knowledge, this is the first study to find altered patterns of hyperactivation-network interactions in individuals with SCD$^+$, who were identified with criteria known to increase their likelihood of developing AD in the future. Hence, this reinforces the hypothesis that the hyperactivation-network interactions described here contribute to identifying individuals in the early disease phase. Furthermore, the different relationships observed between hippocampal versus neocortical patterns of connectivity and memory performance may have implications for therapeutic targets in clinical trials and/or to inform cognitive interventions that could be designed to optimize compensatory mechanisms.

A methodological point that deserves to be discussed at this stage is the potential impact of the enrichment criteria, which incorporated reduced hippocampal volumes and/or *APOE4* genotypes for participants with SCD$^+$(Jessen et al., 2014). Indeed, the intentionally selected genetic enrichment for SCD$^+$ might have had an influence on the patterns of activation and/or connectivity observed in this sample. For instance, it is intriguing that previous reports have found abnormally high levels of hippocampal activation in young *APOE4* carriers (Bondi et al., 2005; Dennis et al., 2010; Filippini et al., 2009; Tran et al., 2017), and one recent study using PLS analysis found patterns of altered memory-related activation in *APOE4* carriers with a family history of AD (Rabipour et al., 2020). Thus, there may be other drivers of hyperactivation and network effects that may not be consistent with the AD causal pathway and have an independent or interactive contribution. Moreover, the fact that we used reduced hippocampal volume as a biomarker of AD may have identified a high reserve subpopulation of individuals with SCD, who demonstrate better cognitive performance than expected given their alleged hippocampal atrophy. Interestingly, a higher level of right temporal activation was suggested to underlie the reserve-related compensatory response to reduce the detrimental effect of hippocampal atrophy on memory performance in individuals at risk of AD (Belleville et al., 2021). This is compatible with our finding that right inferior temporal connectivity was associated with better memory performance in both SCD$^+$ and MCI groups. However, it is important to stress that individuals with SCD$^+$ did not differ from the MCI or control groups on a typical reserve proxy, such as years of formal education.

Although this does not completely exclude a reserve contribution, it nevertheless suggests that it may not be a straightforward account of our findings.

Some limitations must be acknowledged: Given the cross-sectional nature of the study, it was not possible to measure intra-individual longitudinal change in patterns of functional connectivity. Even though genetic and neurodegeneration biomarkers were incorporated to increase the likelihood of future progression in the SCD^{+} group, the classification probably still represents a group of heterogeneous individuals and it is likely that a portion of them will not progress to dementia. Moreover, one particular shortcoming of PLS analysis is the risk of overfitting, as it is designed to maximize correlations between data matrices. Future studies with larger samples will be required to replicate our findings, while directly addressing the issue of overfitting, for instance by performing cross-validation using a validation sample or a split-half procedure. Finally, measures of amyloid or tau were not included, and therefore the sample could not be characterized according to the A/T/N framework (Jack et al., 2016, 2018) and it was not possible to study the relationship between functional connectivity and these AD biomarkers.

5. Conclusions

This study is the first to examine the relationship between hyperactivation, latent patterns of functional connectivity and memory performance in individuals at risk of AD. Our data suggests that hyperactivation relates to a combination of pathological and compensatory patterns of connectivity, depending on the brain area where hyperactivation is observed and disease stage. More specifically, hippocampal hyperactivation and its associated patterns of connectivity appear to relate to the worsening of memory performance. This finding may be related to AD-related pathological processes, while neocortical areas could reflect transient compensatory mechanisms contributing to the maintenance of cognition. These results provide insights on the link between hyperactivation, its associated networks and memory capacity in the early stages of AD, and have implications for early detection as well as therapeutic and cognitive interventions. Longitudinal and multimodal imaging studies will be required for an in-depth understanding of the changes in the functional architecture of the brain and their implication in the fundamental disease processes.

CRediT authorship contribution statement

Nick Corriveau-Lecavalier: Conceptualization, Methodology, Visualization, Project administration, Data curation, Formal analysis, Writing - original draft. **M. Natasha Rajah:** Methodology, Software, Writing - review & editing. **Samira Mellah:** Data curation, Methodology, Writing - review & editing. **Sylvie Belleville:** Conceptualization, Funding acquisition, Methodology, Project administration, Supervision, Writing - review & editing.

Declaration of Competing Interest

The authors declare that they have no known competing financial interests or personal relationships that could have appeared to influence the work reported in this paper.

Acknowledgments

Data used for this research were derived from the CIMA-Q cohort. Hence, several investigators were involved in the development of project design and implementation, and data collection. A list of the CIMA-Q cohort can be found online (http://www.cima-q.ca/). We would like to thank Elizabeth Ankudowich and Charana Rajagopal for their precious advice on data analysis. We would also like to thank Annie Webb for English editing. The CIMA-Q is funded through grants from the Fonds de recherche du Québec - Santé (FRQS), the Pfizer-FQRS Innovation Fund (27239) and Fonds de recherche du Québec (FRQ) cohort funds (279261). SB is funded by a Canadian Institutes of Health Research (CIHR) Foundation grant (154265) and holds a Canada Research Chair in Cognitive Neuroscience of Aging and Brain Plasticity (950-232074). NCL is funded through a doctoral scholarship from CIHR (395361).

Appendix A. Supplementary data

Supplementary data to this article can be found online at https://doi.org/10.1016/j.nicl.2021.102643.

References

Albert, M.S., DeKosky, S.T., Dickson, D., Dubois, B., Feldman, H.H., Fox, N.C., Gamst, A., Holtzman, D.M., Jagust, W.J., Petersen, R.C., Snyder, P.J., Carrillo, M.C., Thies, B., Phelps, C.H., 2011. The diagnosis of mild cognitive impairment due to Alzheimer's disease: recommendations from the National Institute on Aging-Alzheimer's Association workgroups on diagnostic guidelines for Alzheimer's disease. Alzheimer's & dementia 7 (3), 270–279.

Ankudowich, E., Pasvanis, S., Rajah, M.N., 2019. Age-related differences in prefrontal-hippocampal connectivity are associated with reduced spatial context memory. Psychol. Aging 34 (2), 251–261.

Ankudowich, E., Pasvanis, S., Rajah, M.N., 2017. Changes in the correlation between spatial and temporal source memory performance and BOLD activity across the adult lifespan. Cortex 91, 234–249.

Ankudowich, E., Pasvanis, S., Rajah, M.N., 2016. Changes in the modulation of brain activity during context encoding vs. context retrieval across the adult lifespan. NeuroImage 139, 103–113.

Atienza, M., Atalaia-Silva, K.C., Gonzalez-Escamilla, G., Gil-Neciga, E., Suarez-Gonzalez, A., Cantero, J.L., 2011. Associative memory deficits in mild cognitive impairment: the role of hippocampal formation. Neuroimage 57 (4), 1331–1342.

Bai, F., Zhang, Z., Watson, D.R., Yu, H., Shi, Y., Yuan, Y., Qian, Y., 2009. Abnormal functional connectivity of hippocampus during episodic memory retrieval processing network in amnestic mild cognitive impairment. Biol. Psychiatry 65, 951–958.

Bakker, A., Albert, M.S., Krauss, G., Speck, C.L., Gallagher, M., 2015. Response of the medial temporal lobe network in amnestic mild cognitive impairment to therapeutic intervention assessed by fMRI and memory task performance. NeuroImage: Clinical 7, 688–698.

Bakker, A., Krauss, G., Albert, M., Speck, C., Jones, L., Stark, C., Yassa, M., Bassett, S., Shelton, A., Gallagher, M., 2012. Reduction of hippocampal hyperactivity improves cognition in amnestic mild cognitive impairment. Neuron 74 (3), 467–474.

Belleville, S., Clement, F., Mellah, S., Gilbert, B., Fontaine, F., & Gauthier, S. 2011. Training-related brain plasticity in subjects at risk of developing Alzheimer's disease. Brain, 134:1623-1634.

Belleville, S., LeBlanc, A.C., Kergoat, M.-J., Calon, F., Gaudreau, P., Hébert, S.S., Hudon, C., Leclerc, N., Mechawar, N., Duchesne, S., Gauthier, S., Bellec, P., Belleville, S., Bocti, C., Calon, F., Chertkow, H., Collins, L., Cunnane, S., Duchesne, S., Gaudreau, P., Gauthier, S., Hébert, S.S., Marie-Jeanne-Kergoat, C.H., LeBlanc, A.C., Leclerc, N., Mechawar, N., Philips, N., Soucy, J.-P., Dang Vu, T.T., Verret, L., Villalpando, J.M., 2019. The Consortium for the early identification of Alzheimer's disease–Quebec (CIMA-Q). Alzheimer's & Dementia: Diagnosis Assessment & Dis. Monitor. 11 (1), 787–796.

Belleville, S., Mellah, S., Cloutier, S., Dang-Vu, T.T., Duchesne, S., Maltezos, S., Hudon, C., 2021. Neural correlates of resilience to the effects of hippocampal atrophy on memory. NeuroImage Clin. 29, 102526.

Benoit, R.G., Schacter, D.L., 2015. Specifying the core network supporting episodic simulation and episodic memory by activation likelihood estimation. Neuropsychologia 75, 450–457.

Bero, A.W., Yan, P., Roh, J.H., Cirrito, J.R., Stewart, F.R., Raichle, M.E., Holtzman, D.M., 2011. Neuronal activity regulates the regional vulnerability to amyloid-β deposition. Nat. Neurosci. 14, 750.

Berron, D., Cardenas-Blanco, A., Bittner, D., Metzger, C.D., Spottke, A., Heneka, M.T., Fliessbach, K., Schneider, A., Teipel, S.J., Wagner, M., Speck, O., Jessen, F., Düzel, E., 2019. Higher CSF tau levels are related to hippocampal hyperactivity and object mnemonic discrimination in older adults. J. Neurosci. 39 (44), 8788–8797.

Bischof, G.N., Ewers, M., Franzmeier, N., Grothe, M.J., Hoenig, M., Kocagoncu, E., van Eimeren, T., 2019. Connectomics and molecular imaging in neurodegeneration. Eur. J. Nucl. Med. Mol. Imaging 1–12.

Bondi, M.W., Houston, W.S., Eyler, L.T., Brown, G.G., 2005. fMRI evidence of compensatory mechanisms in older adults at genetic risk for Alzheimer disease. Neurology 64, 501–508.

Busche, M.A., Chen, X., Henning, H.A., Reichwald, J., Staufenbiel, M., Sakmann, B., Konnerth, A., 2012. Critical role of soluble amyloid-β for early hippocampal hyperactivity in a mouse model of Alzheimer's disease. Proc. Natl. Acad. Sci. U.S.A. 109, 8740–8745.

Busche, M.A., Wegmann, S., Dujardin, S., Commins, C., Schiantarelli, J., Klickstein, N., Kamath, T.V., Carlson, G.A., Nelken, I., Hyman, B.T., 2019. Tau impairs neural circuits, dominating amyloid-β effects, in Alzheimer models in vivo. Nat. Neurosci. 22 (1), 57–64.

Celone, K.A., Calhoun, V.D., Dickerson, B.C., Atri, A., Chua, E.F., Miller, S.L., DePeau, K., Rentz, D.M., Selkoe, D.J., Blacker, D., Albert, M.S., Sperling, R.A., 2006. Alterations

in memory networks in mild cognitive impairment and Alzheimer's disease: an independent component analysis. J. Neurosci. 26 (40), 10222–10231.
Chhatwal, J.P., Schultz, A.P., Johnson, K.A., Hedden, T., Jaimes, S., Benzinger, T.L., Ghetti, B., 2018. Preferential degradation of cognitive networks differentiates Alzheimer's disease from ageing. Brain 141, 1486–1500.
Clément, F., Belleville, S., 2010. Compensation and disease severity on the memory-related activations in mild cognitive impairment. Biol. Psychiatry 68 (10), 894–902.
Clément, F., Belleville, S., 2012. Effect of disease severity on neural compensation of item and associative recognition in mild cognitive impairment. J. Alz. Dis. 29 (1), 109–123. https://doi.org/10.3233/JAD-2012-110426.
Clément, F., Belleville, S., Mellah, S., 2010. Functional neuroanatomy of the encoding and retrieval processes of verbal episodic memory in MCI. Cortex 46 (8), 1005–1015.
Clément, F., Gauthier, S., Belleville, S., 2013. Executive functions in mild cognitive impairment: emergence and breakdown of neural plasticity. Cortex 49 (5), 1268–1279.
Corriveau-Lecavalier, N., Duchesne, S., Gauthier, S., Hudon, C., Kergoat, M.-J., Mellah, S., Belleville, S., for the Consortium of early identification of Alzheimer's disease-Quebec (CIMA-Q). 2021. A quadratic function of activation in individuals at risk of Alzheimer's disease. Alzheimer's & Dementia: Diagnosis, Assessment & Disease Monitoring, 12: e12139.
Corriveau-Lecavalier, N., Mellah, S., Clément, F., & Belleville, S. 2019. Evidence of parietal hyperactivation in individuals with mild cognitive impairment who progressed to dementia: A longitudinal fMRI study. NeuroImage: Clinical, 24: 101958.
Dale, A.M., Fischl, B., Sereno, M.I., 1999. Cortical surface-based analysis: I Segmentation and surface reconstruction. Neuroimage 9 (2), 179–194.
Dennis, N.A., Browndyke, J.N., Stokes, J., Need, A., Burke, J.R., Welsh-Bohmer, K.A., Cabeza, R., 2010. Temporal lobe functional activity and connectivity in young adult APOE ε4 carriers. Alzheimer's & Dementia 6, 303–311.
Dickerson, B.C., Salat, D.H., Bates, J.F., Atiya, M., Killiany, R.J., Greve, D.N., Dale, A.M., Stern, C.E., Blacker, D., Albert, M.S., Sperling, R.A., 2004. Medial temporal lobe function and structure in mild cognitive impairment. Ann. Neurol. 56 (1), 27–35.
Dickerson, B.C., Salat, D.H., Greve, D.N., Chua, E.F., Rand-Giovannetti, E., Rentz, D.M., Albert, M.S., 2005. Increased hippocampal activation in mild cognitive impairment compared to normal aging and AD. Neurology 65, 404–411.
Duchesne, S., Chouinard, I., Potvin, O., Fonov, V.S., Khademi, A., Bartha, R., Bellec, P., Collins, D.L., Descoteaux, M., Hoge, R., McCreary, C.R., Ramirez, J., Scott, C.J.M., Smith, E.E., Strother, S.C., Black, S.E., 2019. The Canadian dementia imaging protocol: harmonizing national cohorts. J. Magn. Reson. Imaging 49 (2), 456–465.
Elman, J.A., Oh, H., Madison, C.M., Baker, S.L., Vogel, J.W., Marks, S.M., Crowley, S., O'Neil, J.P., Jagust, W.J., 2014. Neural compensation in older people with brain amyloid-β deposition. Nat. Neurosci. 17 (10), 1316–1318.
Elshiekh, A., Subramaniapillai, S., Rajagopal, S., Pasvanis, S., Ankudowich, E., Rajah, M. N., 2020. The association between cognitive reserve and performance-related brain activity during episodic encoding and retrieval across the adult lifespan. Cortex 129, 296–313.
Erk, S., Spottke, A., Meisen, A., Wagner, M., Walter, H., Jessen, F., 2011. Evidence of neuronal compensation during episodic memory in subjective memory impairment. Arch. Gen. Psychiatry 68, 845–852.
Franzmeier, N., Dewenter, A., Frontzkowski, L., Dichgans, M., Rubinski, A., Neitzel, J., Ewers, M., 2020a. Patient-centered connectivity-based prediction of tau pathology spread in Alzheimer's disease. Sci. Adv. 6, eabd1327.
Franzmeier, N., Neitzel, J., Rubinski, A., Smith, R., Strandberg, O., Ossenkoppele, R., Ewers, M., 2020b. Functional brain architecture is associated with the rate of tau accumulation in Alzheimer's disease. Nat. Commun. 11, 1–17.
Franzmeier, N., Rubinski, A., Neitzel, J., Kim, Y., Damm, A., Na, D. L., ... & Duering, M. 2019. Functional connectivity associated with tau levels in ageing, Alzheimer's, and small vessel disease. Brain, 142:1093-1107.
Filippini, N., MacIntosh, B.J., Hough, M.G., Goodwin, G.M., Frisoni, G.B., Smith, S.M., Mackay, C.E., 2009. Distinct patterns of brain activity in young carriers of the APOE-ε4 allele. Proc. Natl. Acad. Sci. U.S.A. 106, 7209–7214.
Greicius, M.D., Srivastava, G., Reiss, A.L., Menon, V., 2004. Default-mode network activity distinguishes Alzheimer's disease from healthy aging: evidence from functional MRI. Proc. Natl. Acad. Sci. 101 (13), 4636–4642. https://doi.org/10.1073/pnas.0308627101.
Hallinan, G.I., Vargas-Caballero, M., West, J., Deinhardt, K., 2019. Tau misfolding efficiently propagates between individual intact hippocampal neurons. J. Neurosci. 39 (48), 9623–9632.
Huijbers, W., Mormino, E.C., Schultz, A.P., Wigman, S., Ward, A.M., Larvie, M., Sperling, R.A., 2015. Amyloid-β deposition in mild cognitive impairment is associated with increased hippocampal activity, atrophy and clinical progression. Brain 138, 1023–1035.
Huijbers, W., Schultz, A.P., Papp, K.V., LaPoint, M.R., Hanseeuw, B., Chhatwal, J.P., Hedden, T., Johnson, K.A., Sperling, R.A., 2019. Tau accumulation in clinically normal older adults is associated with hippocampal hyperactivity. J. Neurosci. 39 (3), 548–556.
Jacobs, H.I.L., Radua, J., Lückmann, H.C., Sack, A.T., 2013. Meta-analysis of functional network alterations in Alzheimer's disease: toward a network biomarker. Neurosci. Biobehav. Rev. 37 (5), 753–765.
Jessen, F., Amariglio, R.E., Buckley, R.F., van der Flier, W.M., Han, Y., Molinuevo, J.L., Rabin, L., Rentz, D.M., Rodriguez-Gomez, O., Saykin, A.J., Sikkes, S.A.M., Smart, C. M., Wolfsgruber, S., Wagner, M., 2020. The characterisation of subjective cognitive decline. Lancet Neurol. 19 (3), 271–278.
Jessen, F., Amariglio, R.E., van Boxtel, M., Breteler, M., Ceccaldi, M., Chételat, G., Dubois, B., Dufouil, C., Ellis, K.A., van der Flier, W.M., Glodzik, L., van Harten, A.C., de Leon, M.J., McHugh, P., Mielke, M.M., Molinuevo, J.L., Mosconi, L., Osorio, R.S., Perrotin, A., Petersen, R.C., Rabin, L.A., Rami, L., Reisberg, B., Rentz, D.M., Sachdev, P.S., de la Sayette, V., Saykin, A.J., Scheltens, P., Shulman, M.B., Slavin, M. J., Sperling, R.A., Stewart, R., Uspenskaya, O., Vellas, B., Visser, P.J., Wagner, M., 2014. A conceptual framework for research on subjective cognitive decline in preclinical Alzheimer's disease. Alzheimer's & dementia 10 (6), 844–852.
Jack Jr, C.R., Bennett, D.A., Blennow, K., Carrillo, M.C., Dunn, B., Sperlig, R.A., 2018. NIA-AA research framework: toward a biological definition of Alzheimer's disease. Alzheimer's & Dementia 14, 535–562.
Jack Jr, C.R., Bennett, D.A., Blennow, K., Carrillo, M.C., Feldman, Dubois, B., 2016. A/T/N: an unbiased descriptive classification scheme for Alzheimer disease biomarkers. Neurology 87, 539–547.
Jones, David T., Graff-Radford, Jonathan, Lowe, Val J., Wiste, Heather J., Gunter, Jeffrey L., Senjem, Matthew L., Botha, Hugo, Kantarci, Kejal, Boeve, Bradley F., Knopman, David S., Petersen, Ronald C., Jack, Clifford R., 2017. Tau, amyloid, and cascading network failure across the Alzheimer's disease spectrum. Cortex 97, 143–159.
Jones, David T., Knopman, David S., Gunter, Jeffrey L., Graff-Radford, Jonathan, Vemuri, Prashanthi, Boeve, Bradley F., Petersen, Ronald C., Weiner, Michael W., Jack, Clifford R., 2016. Cascading network failure across the Alzheimer's disease spectrum. Brain 139 (2), 547–562.
Jones, D.T., Machulda, M.M., Vemuri, P., McDade, E.M., Zeng, G., Senjem, M.L., Boeve, B.F., 2011. Age-related changes in the default mode network are more advanced in Alzheimer disease. Neurology 77, 1524–1531.
Kim, H. R., Lee, P., Seo, S. W., Roh, J. H., Oh, M., Oh, J. S., ... & Jeong, Y. 2019. Comparison of Amyloid β and Tau Spread Models in Alzheimer's Disease. Cerebral Cortex, 29:4291-4302.
Kircher, T.T., Weis, S., Freymann, K., Erb, M., Jessen, F., Grodd, W., Leube, D.T., 2007. Hippocampal activation in patients with mild cognitive impairment is necessary for successful memory encoding. J. Neurol. Neurosurg. Psychiatry 78, 812–818.
Krishnan, Anjali, Williams, Lynne J., McIntosh, Anthony Randal, Abdi, Hervé, 2011. Partial Least Squares (PLS) methods for neuroimaging: a tutorial and review. Neuroimage 56 (2), 455–475.
Leal, S.L., Landau, S.M., Bell, R.K., Jagust, W.J., 2017. Hippocampal activation is associated with longitudinal amyloid accumulation and cognitive decline. Elife 6, e22978. https://doi.org/10.7554/eLife.22978.001.
Marks, Shawn M., Lockhart, Samuel N., Baker, Suzanne L., Jagust, William J., 2017. Tau and β-amyloid are associated with medial temporal lobe structure, function, and memory encoding in normal aging. J. Neurosci. 37 (12), 3192–3201.
McIntosh, Anthony Randal, Lobaugh, Nancy J., 2004. Partial least squares analysis of neuroimaging data: applications and advances. Neuroimage 23, S250–S263.
Mormino, E.C., Brandel, M.G., Madison, C.M., Marks, S., Baker, S.L., Jagust, W.J., 2012. Aβ deposition in aging is associated with increases in brain activation during successful memory encoding. Cereb. Cortex 22, 1813–1823.
Morris, John C., 1997. Clinical dementia rating: a reliable and valid diagnostic and staging measure for dementia of the Alzheimer type. Int. Psychogeriatr. 9 (S1), 173–176.
Nasreddine, Z. S., Phillips, N. A., Bédirian, V., Charbonneau, S., Whitehead, V., Collin, I., ... & Chertkow, H. 2005. The Montreal Cognitive Assessment, MoCA: a brief screening tool for mild cognitive impairment. Journal of the American Geriatrics Society, 53:695-699.
Pasquini, Lorenzo, Rahmani, Farzaneh, Maleki-Balajoo, Somayeh, La Joie, Renaud, Zarei, Mojtaba, Sorg, Christian, Drzezga, Alexander, Tahmasian, Masoud, 2019. Medial temporal lobe disconnection and hyperexcitability across alzheimer's disease stages. J. Alzheimer's Dis. Rep. 3 (1), 103–112.
Putcha, D., Brickhouse, M., O'Keefe, K., Sullivan, C., Rentz, D., Marshall, G., Dickerson, B., Sperling, R., 2011. Hippocampal hyperactivation associated with cortical thinning in Alzheimer's disease signature regions in non-demented elderly adults. J. Neurosci. 31 (48), 17680–17688.
Rabipour, S., Rajagopal, S., Yu, E., Pasvanis, S., Lafaille-Magnan, M. E., Breitner, J., ... & PREVENT-AD Research Group. (2020). APOE4 Status is Related to Differences in Memory-Related Brain Function in Asymptomatic Older Adults with Family History of Alzheimer's Disease: Baseline Analysis of the PREVENT-AD Task Functional MRI Dataset. Journal of Alzheimer's Disease, (Preprint), 1-23.
Richetin, K., Steullet, P., Pachoud, M., Perbet, R., Parietti, E., Maheswaran, M., Déglon, N., 2020. Tau accumulation in astrocytes of the dentate gyrus induces neuronal dysfunction and memory deficits in Alzheimer's disease. Nat. Neurosci. 23, 1567–1579.
Rodda, J.E., Dannhauser, T.M., Cutinha, D.J., Shergill, S.S., Walker, Z., 2009. Subjective cognitive impairment: increased prefrontal cortex activation compared to controls during an encoding task. Int. J. Geriat. Psychiatry J. Psychiatry Late Life Allied Sci. 24, 865–874.
Rodda, J., Dannhauser, T., Cutinha, D.J., Shergill, S.S., Walker, Z., 2011. Subjective cognitive impairment: functional MRI during a divided attention task. Eur. Psychiatry 26 (7), 457–462.
Schultz, Aaron P., Chhatwal, Jasmeer P., Hedden, Trey, Mormino, Elizabeth C., Hanseeuw, Bernard J., Sepulcre, Jorge, Huijbers, Willem, LaPoint, Molly, Buckley, Rachel F., Johnson, Keith A., Sperling, Reisa A., 2017. Phases of hyperconnectivity and hypoconnectivity in the default mode and salience networks track with amyloid and tau in clinically normal individuals. J. Neurosci. 37 (16), 4323–4331.
Sepulcre, Jorge, Sabuncu, Mert R., Li, Quanzheng, El Fakhri, Georges, Sperling, Reisa, Johnson, Keith A., 2017. Tau and amyloid β proteins distinctively associate to functional network changes in the aging brain. Alzheimer's & Dementia 13 (11), 1261–1269.
Sperling, Reisa A., Aisen, Paul S., Beckett, Laurel A., Bennett, David A., Craft, Suzanne, Fagan, Anne M., Iwatsubo, Takeshi, Jack, Clifford R., Kaye, Jeffrey,

Montine, Thomas J., Park, Denise C., Reiman, Eric M., Rowe, Christopher C., Siemers, Eric, Stern, Yaakov, Yaffe, Kristine, Carrillo, Maria C., Thies, Bill, Morrison-Bogorad, Marcelle, Wagster, Molly V., Phelps, Creighton H., 2011. Toward defining the preclinical stages of Alzheimer's disease: Recommendations from the National Institute on Aging-Alzheimer's Association workgroups on diagnostic guidelines for Alzheimer's disease. Alzheimer's & Dementia 7 (3), 280–292.

Sperling, Reisa A., Dickerson, Bradford C., Pihlajamaki, Maija, Vannini, Patrizia, LaViolette, Peter S., Vitolo, Ottavio V., Hedden, Trey, Alex Becker, J., Rentz, Dorene M., Selkoe, Dennis J., Johnson, Keith A., 2010. Functional alterations in memory networks in early Alzheimer's disease. NeuroMol. Med. 12 (1), 27–43.

Tran, T.T., Speck, C.L., Pisupati, A., Gallagher, M., Bakker, A., 2017. Increased hippocampal activation in ApoE-4 carriers and non-carriers with amnestic mild cognitive impairment. NeuroImage: Clin. 13, 237–245.

Troyer, Angela K., Murphy, Kelly J., Anderson, Nicole D., Hayman-Abello, Brent A., Craik, Fergus I.M., Moscovitch, Morris, 2008. Item and associative memory in amnestic mild cognitive impairment: performance on standardized memory tests. Neuropsychology 22 (1), 10–16.

Vogel, J.W., Iturria-Medina, Y., Strandberg, O.T., Smith, R., Levitis, E., Evans, A.C., Hansson, O., 2020. Spread of pathological tau proteins through communicating neurons in human Alzheimer's disease. Nat. Commun. 11, 1–15.

Wechsler, D., 1987. Wechsler Memory Scale-Revised. Psychological Corporation.

Wilke, M., 2012. An alternative approach towards assessing and accounting for individual motion in fMRI timeseries. Neuroimage 59, 2062–2072.

Wilke, M., 2014. Isolated assessment of translation or rotation severely underestimates the effects of subject motion in fMRI data. PLoS ONE 9, e106498.

Wu, J.W., Hussaini, S.A., Bastille, I.M., Rodriguez, G.A., Mrejeru, A., Rilett, K., Herman, M., 2016. Neuronal activity enhances tau propagation and tau pathology in vivo. Nat. Neurosci. 19, 1085.

Yassa, M.A., Lacy, J.W., Stark, S.M., Albert, M.S., Gallagher, M., Stark, C.E., 2011. Pattern separation deficits associated with increased hippocampal CA3 and dentate gyrus activity in nondemented older adults. Hippocampus 21, 968–979.

Zott, B., Busche, M.A., Sperling, R.A., Konnerth, A., 2018. What Happens with the Circuit in Alzheimer's disease in mice and humans? Annu. Rev. Neurosci. 41, 277–297.

Zott, B., Simon, M.M., Hong, W., Unger, F., Chen-Engerer, H.J., Frosch, M.P., Konnerth, A., 2019. A vicious cycle of β amyloid–dependent neuronal hyperactivation. Science 365, 559–565.